ARTICLE
Journal of Cellular Biochemistry 115:1101–1111 (2014)

Journal of Cellular Biochemistry

Sulfated Glycosaminoglycans Support Osteoblast Functions and Concurrently Suppress Osteoclasts

Juliane Salbach-Hirsch,[1] Nicole Ziegler,[1] Sylvia Thiele,[1] Stephanie Moeller,[2] Matthias Schnabelrauch,[2] Vera Hintze,[3] Dieter Scharnweber,[3,4] Martina Rauner,[1] and Lorenz C. Hofbauer[1,4]*

[1]*Dresden Technical University Medical Center, Dresden, Germany*

[2]*Biomaterials Department, INNOVENT e. V, Jena, Germany*

[3]*Institute of Materials Science, Max Bergmann Center of Biomaterials, Technische Universität Dresden, Dresden, Germany*

[4]*Center for Regenerative Therapies Dresden, Dresden, Germany*

ABSTRACT

In order to improve bone regeneration, development and evaluation of new adaptive biomaterials is warranted. Glycosaminoglycans (GAGs) such as hyaluronan (HA) and chondroitin sulfate (CS) are major extracellular matrix (ECM) components of bone, and display osteogenic properties that are potentially useful for biomaterial applications. Using native and synthetic sulfate-modified GAGs, we manufactured artificial collagen/GAG ECM (aECMs) coatings, and evaluated how the presence of GAGs and their degree of sulfation affects the differentiation of murine mesenchymal stem cells to osteoblasts (OB) cultivated on these aECMs. GAG sulfation regulated osteogenesis at all key steps of OB development. Adhesion, but not migration, was diminished by 50% ($P < 0.001$). Proliferation and metabolic activity were slightly ($P < 0.05$) and cell death events strongly ($P < 0.001$) down-regulated due to a switch from proliferative to matrix synthesis state. When exposed to sulfated GAGs, OB marker genes, such as alkaline phosphatase, osteoprotegerin (OPG), and osteocalcin increased by up to 28-fold ($P < 0.05$) and calcium deposition up to 4-fold ($P < 0.05$). Furthermore, GAG treatment of OBs suppressed their ability to support osteoclast (OC) differentiation and resorption. In conclusion, GAG sulfation controls bone cell homeostasis by concurrently promoting osteogenesis and suppressing their paracrine support of OC functions, thus displaying a favorable profile on bone remodeling. Whether these cellular properties translate into improved bone regeneration needs to be validated in vivo. J. Cell. Biochem. 115: 1101–1111, 2014.

KEY WORDS: OSTEOBLASTS (OB); OSTEOCLASTS (OC); HYALURONIC ACID/HYALURONAN (HA) SULFATE; CHONDROITIN SULFATE (CS); GLYCOSAMINOGLYCANS (GAG)

To date, bone grafts are one of the most demanded implant materials [Mathieu et al., 2006]. Delayed or complete failure of osseointegration occurs in 5–20% of the 4 million annually applied bone substitute materials [Brydone et al., 2010], emphasizing the medical and socioeconomic importance for continuous research in this field. High impact medical advances are further increasing the age of implant recipients, creating new challenges for biomaterial design. Implants are used in defective or osteoporotic bone or in patients with comorbidities, such as diabetes mellitus, that may further impair osseointegration [Hench, 1998]. Successful osseointegration of implants depends on the characteristics and regenerative capacity of the host bone as well as material properties. Ongoing developments are therefore directed towards adaptive implant materials instead of the solely inert and mechanosupportive materials of the first generation [Brydone et al., 2010]. Thus, immobilization of components of the native extracellular matrix (ECM) onto established materials is a promising approach because these surfaces mimic the native ECM. Protein adsorption layers formed on these artificial ECMs (aECMs) are likely to be similar to those formed under physiological conditions [Bierbaum et al., 2006].

The ECM of bone consists largely of inorganic mineral and 20–40% organic components of which type I collagen (Coll) with embedded proteoglycans, glycosaminoglycans (GAGs) and other proteins are predominant [Robey and Boskey, 2009]. Local GAGs consist of about 90% chondroitin sulfate (CS), and small amounts of hyaluronan (HA) and dermatan sulfate [Prince and Navia, 1983]. These polymers

All listed institutions were involved in this studies execution of experiments.
Grant sponsor: Deutsche Forschungsgemeinschaft; Grant numbers: TRR67-B2, TRR67-A2, TRR67-A3.
*Correspondence to: Lorenz C Hofbauer, Universitätsklinikum "Carl Gustav Carus", Fetscherstraße 74, Dresden 01307, Germany. E-mail: lorenz.hofbauer@uniklinikum-dresden.de
Manuscript Received: 1 November 2013; Manuscript Accepted: 12 December 2013
Accepted manuscript online in Wiley Online Library (wileyonlinelibrary.com): 19 December 2013
DOI 10.1002/jcb.24750 • © 2013 Wiley Periodicals, Inc.

have been utilized in their native form in Coll/GAG composites for medical applications since the 1970s [Spector, 2013], but only limited conclusive knowledge on the cellular interactions at the bone graft-host interface is available and more in depth research is required.

Physiological bone regeneration is a coordinated process, maintained by bone-forming osteoblasts and bone-resorbing osteoclasts. Recently, we reported that the sulfate modification of GAGs in Coll/GAG coatings might be a promising tool to regulate biological processes at the bone/biomaterial interface. The sulfate modification of GAGs profoundly inhibits OC differentiation and their resorptive capacity [Salbach et al., 2012a]. Furthermore, OPG directly interacts with sulfated GAGs resulting in an altered OPG bioactivity [Salbach-Hirsch et al., 2013]. Therefore, GAGs hold a great potential for the development of innovative biomimetic materials for bone tissue engineering applications and regenerative medicine [Pichert et al., 2012].

Here we tested the hypothesis whether sulfate modification of GAGs in Coll/GAG aECMs also affects the osteogenic differentiation of MSCs, osteoblast activity and their paracrine regulation of OC functionality. Since dexamethasone (Dex), an essential supplement for human MSC differentiation [Pittenger, 2008], induces variable cell behaviors in vitro [Hempel et al., 2012] our study was performed in a murine model without Dex to avoid this confounder.

Our data show that GAG sulfation promotes osteogenesis and suppresses the osteoblastic support of osteoclast differentiation and bone resorption.

MATERIALS AND METHODS

MATERIALS

Native, high-molecular weight hyaluronan (HA, from streptococcus, $M_W = 1{,}175{,}000\ gmol^{-1}$) was purchased from Aqua Biochem (Dessau, Germany), chondroitin sulfate (CS, porcine trachea, a mixture of 70% chondroitin-4-sulfate and 30% chondroitin-6-sulfate, degree of sulfation (DS_S) = 0.9, Mw = 20,000 $gmol^{-1}$) from Kraeber (Ellerbek, Germany). The fluorescent dye ATTO 565-NH_2 ($\lambda_{abs} = 563$ nm) was supplied by ATTO-TEC (Siegen, Germany), 1-ethyl-3-(3-dimethylaminopropyl) carbodiimide hydrochloride (EDC) and *N*-hydroxysuccinimide (NHS) were available from Sigma–Aldrich (Taufkirchen, Germany).

PREPARATION OF GAG DERIVATIVES AND ARTIFICIAL ECMs (aECMs)

A thermally degraded, low molecular weight HA (HA_{LMW}) was used as a reference in addition to the full-length HA since its molecular weight (M_w) is known to significantly decrease during the sulfation process [Hintze et al., 2009]. HA_{LMW} ($M_w = 132{,}200\ gmol^{-1}$) was prepared via controlled thermal degradation of the native high-molecular weight HA according to the literature [Kunze et al., 2010] and characterized as previously specified [Salbach et al., 2012a].

The sulfated CS and HA GAG derivatives (sCS3, $DS_S = 3.0$, $M_W = 26{,}800\ gmol^{-1}$; sHA3, $DS_S = 3.1$; $M_W = 53{,}300\ gmol^{-1}$) for aECM preparation were synthesized and characterized as previously described [Salbach et al., 2012a].

Artificial ECMs were derived by in vitro fibrillogenesis of rat Coll type I in the presence of HA, sHA3, HA_{LMW}, CS, or sCS3 as described in our previous publication [Salbach et al., 2012a]. If not stated otherwise, cells were differentiated on these aECMs.

For uptake tracking of GAGs into cells, a fluorescence labeling was performed to the GAG derivatives. We incorporated a rhodamine-type fluorescent dye (ATTO 565) into HA derivatives using two different procedures. Following a conventional EDC/NHS coupling protocol an amino group containing ATTO 565 derivative (ATTO 565-NH_2) was coupled onto the carboxyl groups of HA_{LMW} (side-on-functionalization). A different procedure was employed for the sHA3 labeling to avoid impairment of the coupling by the previously introduced sulfate groups. The ATTO 565-NH_2 was coupled to the reducing end of the GAG via an azomethine structure which was subsequently reduced by $NaBH_3CN$ resulting in the more stable amine derivative (end-on-functionalization). A schematic representation of the different fluorescence labeled polymer structures is given in Figure 1.

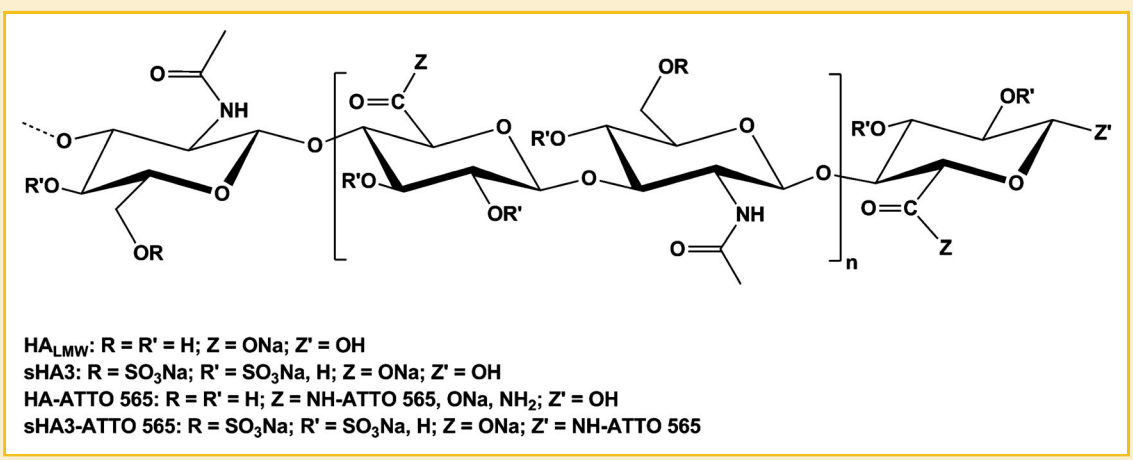

Fig. 1. Structural characteristics of HA derivatives. For immunofluorescence, HA_{LMW} and sHA3 were functionalized with a red fluorescent ATTO 565 group either by side-on or end-on functionalization. The given scheme depicts HA and sHA3 and the location of the introduced dye within the two polymers.

The exact labeling procedure was performed as follows:

ATTO 565-labeled HA_{LMW} (HA-ATTO 565): 1.25 mmol EDC were added to 0.62 mmol HA_{LMW} ($M_w = 23{,}200\ gmol^{-1}$) dissolved in distilled water. The pH was adjusted to 4.75 using 1 M HCl and the mixture was stirred for 30 min at room temperature (RT). Subsequently, 1.25 mmol NHS were added. Then 0.7 μmol of ATTO 565-NH_2, dissolved in dimethyl sulfoxide (DMSO), were added to the polymer mixture and stirred at RT for 4 h. The remaining free active carboxyl groups were saturated using ammonia and stirring for 2 h. The GAG was purified by dialysis against distilled water, followed by lyophilization under vacuum. Yield: 75%.

To avoid impairment of the coupling by the previously induced sulfate groups a different procedure was employed for the sHA3 labeling.

ATTO 565-labeled sHA3 (sHA3-ATTO 565): 0.7 μmol ATTO 565-NH_2 (dissolved in DMSO) were added to 0.33 mmol sHA3 ($DS_S = 3.6$, $M_w = 28\,600\ gmol^{-1}$) dissolved in distilled water and reaction mixture was stirred at RT for 6 h. Then 0.65 mmol $NaBH_3CN$ were added to the solution, and after stirring for 72 h, the product was purified as described above. Yield: 90%.

CELL CULTURE OF MURINE OBs AND OCs

Murine OBs were generated from mesenchymal stromal cells (MSC) flushed from the femora bone marrow of healthy wild type mice. After isolation, cells were plated and maintained in basal medium consisting of MEM-α (Biochrom, Hagen, Germany) supplemented with 10% FCS (PAA, Cölbe, Germany), 1% penicillin/streptomycin (Gibco, Darmstadt, Germany) and 2 mM glutamine (Biochrom) in 75 cm^2 cell culture flasks. MSCs were detached using trypsin (PAA), transferred to aECM-coated well plates or flasks and differentiated with 100 μM ascorbate phosphate (Sigma–Aldrich) and 10 mM β-glycerol phosphate (Sigma–Aldrich) for up to 21 days until further analysis. Media was exchanged every 48 h and stored at −80°C for subsequent OC culture in OB-conditioned medium.

Murine monocytic RAW264.7 cells (TIB-71™, ATCC, Wesel, Germany) that served as model for OCs, were cultured up to 85% confluency in basal medium until splitting or utilization in co-culture experiments.

INDIRECT CO-CULTURE OF OCs AND OBs

To further analyze the impact of GAG modifications on OB-to-OC signaling, supernatants of OB experiments were applied to OC cultures. In brief, 12,500 RAW264.7 cells/cm^2 were seeded into uncoated well plates containing OB-derived conditioned medium and stimulated with RANKL (10 ng/ml, R&D Systems, Wiesbaden-Nordenstadt, Germany) to counter the excessive OPG exceeding 1,200 pg/ml (ELISA, data not shown) and initiate the generation of multinuclear OCs within 4 days.

SUSCEPTIBILITY TO GAGs

MSCs were seeded on uncoated glass slides and incubated with 1 mg/ml HA-ATTO 565 or sHA3-ATTO 565 for up to 24 h to determine (i) if MSCs internalize both, the native and the high-sulfated, forms of HAs or if the interaction occurs only at the membrane, (ii) where these HAs are localized in cells, and (iii) if there are kinetic differences of internalization. After the incubation period, slides were stained for fibrillar actin and cell nuclei, as previously described [Salbach et al., 2012a]. Cells cultured without HAs served as control.

ADHESION OF PRECURSOR CELLS

Adhesion of 0.3×10^6 MSCs or 0.8×10^6 RAW264.7 cells/cm^2 to the various aECMs or to supernatant-containing well plates was assessed after 1 h. To ensure cell surface receptor integrity, cells were detached with 0.25% EDTA (Serva, Heidelberg, Germany) in HBSS (PAA). After 60 min non-adherent cells were removed with PBS. The remaining cells were stained with 0.04% crystal violet (Sigma–Aldrich) in 4% ethanol (VWR, Darmstadt, Germany) for 30 min. After extensive washing with water, the plates were dried. Afterwards, the incorporated dye was dissolved using 1% SDS (Carl Roth, Karlsruhe, Germany), transferred into a 96-well plate, and quantified by measuring the absorbance at 595 nm.

METABOLIC ACTIVITY

Dehydrogenase activity, as an indicator for cell viability, was assessed using a commercial assay (CellTiterBlue®, Promega, Mannheim, Germany). Cells were cultured for 5 days (MSCs) on aECM-coated 48-well plates or 24 h in the presence of conditioned media (RAW264.7), respectively. Then, medium was exchanged for fresh medium containing the resazurin dye, and viability was determined by the ability of living cells to convert resazurin dye into a fluorescent product. Fluorescence intensity was quantified using FluoStar Omega (560Ex/590Em nm, BMG Labtech, Ortenberg, Germany). To further analyze the underlying mechanisms apoptosis, necrosis, and cell proliferation were assessed.

PROLIFERATION ASSAY

Proliferation was measured using a BrdU ELISA (Cell Proliferation ELISA, BrdU [colorimetric], Roche) as described in the manufacturer's instructions. BrdU labeling solution was added to the cell culture 24 h prior to analysis that detects the pyrimidine analogue BrdU incorporated into the DNA of proliferating cells.

CELL DEATH ASSAY

Apoptosis and necrosis were analyzed using the Cell Death Detection ELISA^{PLUS} kit (Roche, Mannheim, Germany). This assay detects mono- and oligo-nucleosomes in supernatants and the cytoplasmic fraction of cell lysates and was performed at the same time points as the viability measurements described above.

ALKALINE PHOSPHATASE (ALP) ACTIVITY AND MINERALIZATION ASSAY

ALP activity and mineralization were assessed as markers for early and late differentiation of OBs after 7 or 21 days of culture as previously described [Rauner et al., 2009]. In brief, at day 7 cell lysates were incubated with an ALP substrate buffer (100 mM diethanolamine, 150 mM NaCl, 2 mM $MgCl_2$, and 2.5 μg/ml *p*-nitrophenylphosphate). Colour change was measured via spectrometer and normalized to total protein concentration.

To determine mineral deposition cells were fixed at day 21 with 70% ethanol and stained with 40 mM alizarin red S. Excess dye was removed by washing with distilled water. Plates were dried and the residual bound and stained calcium was then eluted using 100 mM

cetylpyridinium chloride and quantified with a spectrometer at 540 nm.

OSTEOCLAST FORMATION

Following differentiation in conditioned media for 4 days, RAW264.7 cells were stained for tartrate-resistant acid-phosphatase (TRAP) using the assay kit from Sigma–Aldrich. The differentiation of OCs was determined by counting the number of multinucleated ($\geq$3 nuclei) TRAP-positive cells in each well.

OSTEOCLAST RESORPTIVE ACTIVITY

OC resorption activity was examined using a novel functional resorption assay [Lutter et al., 2010]. RAW264.7 cells were plated on SaOS2-derived matrix and differentiated in the presence or absence of OB-conditioned media (cells grown on aECMs) until distinct resorption pits could be observed. To examine the residual matrix, plates were stained with *von Kossa* which detects both changes in mineral and organic moieties. Images were analyzed and quantified by pixel analysis using ImageJ [Salbach et al., 2012a; Schneider et al., 2012].

CELL MIGRATION

The migration potential of primary MSCs in the presence of various solute GAGs, and of RAW264.7 cells in OB-conditioned medium (cells grown on aECMs) was assessed using the Oris^{TM} Cell Migration (Platypus Technologies, Hamburg, Germany) assay. To block cell proliferation, mitomycin C (Calbiochem, Darmstadt, Germany) was applied at 10 μg/ml for 2.5 h prior to the start of the experiment and again after each day of culture. Pictures were taken every 24 h and lateral ingrowth calculated using ImageJ software [Schneider et al., 2012].

RNA ISOLATION, REVERSE TRANSCRIPTION, AND QUANTITATIVE REAL TIME PCR

RNA extraction, reverse transcription, and real time PCR were performed as previously described [Salbach et al., 2012a]. Primer sequences for the analyzed genes are given in Table I. The abundance of mRNA levels was calculated using the $\Delta\Delta$-c_t-method [Livak and Schmittgen, 2001] and is presented in fold increase relative to the respective control. ALP expression was assessed as an early differentiation marker, osteocalcin (OCN) as late differentiation marker, and runt-related transcription factor 2 (Runx2) as a major osteoblastic transcription factor.

TABLE I. Synoptic Overview of all Primers Used in This Study

Primer	Sequence 5′ → 3′
β-Actin s	GATCTGGCACCACACCTTCT
β-Actin as	GGGGTGTTGAAGGTCTCAAA
RANKL s	CACTGAGGAGACCACCCAAG
RANKL as	GAGATGAAGAGGAGCAGAACG
OPG s	CCTTGCCCTGACCACTCTTA
OPG as	ACACTGGGCTGCAATACACA
ALP s	GAAAGCAGGGAAGTCTGTGG
ALP as	AGATGAGTTGAGTGGCGATG
Runx2 s	CCCAGCCACCTTTACCTACA
Runx2 as	TATGGAGTGCTGCTGGTCTG
OCN s	GCGCTCTGTCTCTCTGACCT
OCN as	ACCTTATTGCCCTCCTGCTT

STATISTICAL ANALYSIS

All experiments were performed at least in triplicate and evaluated using one-way ANOVA. Exact number of replicates is given in each figure legend. Single data points were excluded after an extreme studentized deviate test confirmed the presence of a significant outlier (Grubb's test). Student's *t*-test was performed to evaluate differences between the treatment groups. All results are presented as normalized mean ± SD. *P*-values < 0.05 were considered statistically significant.

RESULTS

MSCs ARE SUSCEPTIBLE TO NATIVE AND SULFATED GAGs

The following study aimed to characterize the suitability of Coll/GAG coatings for biomaterial application. Analysis was therefore carried out for processes that contribute to the regulatory potential at material/biological system interfaces starting as early as cellular uptake of GAGs and attachment and migration of OB and OC precursors in response to the presence and sulfate modification of GAGs.

MSCs showed susceptibility for unsulfated HA-ATTO 565 and sulfated sHA3-ATTO 565 (Fig. 2). Upon exposure, the GAGs initially showed a diffuse distribution in the cytoplasm. Of note, the apparent higher fluorescent intensity of the sHA3-ATTO 565 at early time-points does not necessarily mirror higher or faster uptake, since fluorescence intensity of both derivatives was unmatched. Uptake velocity was therefore rated by the formation of GAG containing vesicles, which were observed in the perinuclear region of cells exposed to both HAs after 24 h. Vesicle formation occurred after 1 h for the HA-ATTO 565, whereas vesicles of sHA3-ATTO 565 did not appear before 6 h (Fig. 2, white arrows). In general, cells with internalized GAGs showed abnormal morphology devoid of stress fibers.

GAGs MODULATE INITIAL CELL ADHESION, BUT NOT MIGRATION

Similar to our previous observations on OC precursors [Salbach et al., 2012a], initial cell adhesion of murine MSCs was altered in the presence of matrices containing sulfated, but not native, GAGs. Here, sulfation resulted in decreased MSC adhesion, with no differences between the HA or CS derivatives (Fig. 3A). However, no significant differences in cell migration were detected in response to soluble GAG treatment over a time course of 72 h (Fig. 3B).

GAG SULFATION IS A REGULATOR OF OSTEOBLAST METABOLIC ACTIVITY

Exposure to matrices containing high-sulfated GAGs led to a minor decrease in metabolic activity of murine MSCs compared to their native or non-sulfated counter parts (Fig. 4A CS vs. sCS3; HA_{LMW} vs. sHA3). Those matrices containing native, high-molecular weight HA profoundly increased metabolic activity (Fig. 4A). Concurrent analysis of proliferation (Fig. 4B), necrosis (Fig. 4C), and apoptosis (Fig. 4D) revealed that GAG chain length modulated both proliferation and metabolic activity (HA vs. HA_{LMW}). Matrices containing HA or CS did not significantly affect proliferation and necrosis (Fig. 4B

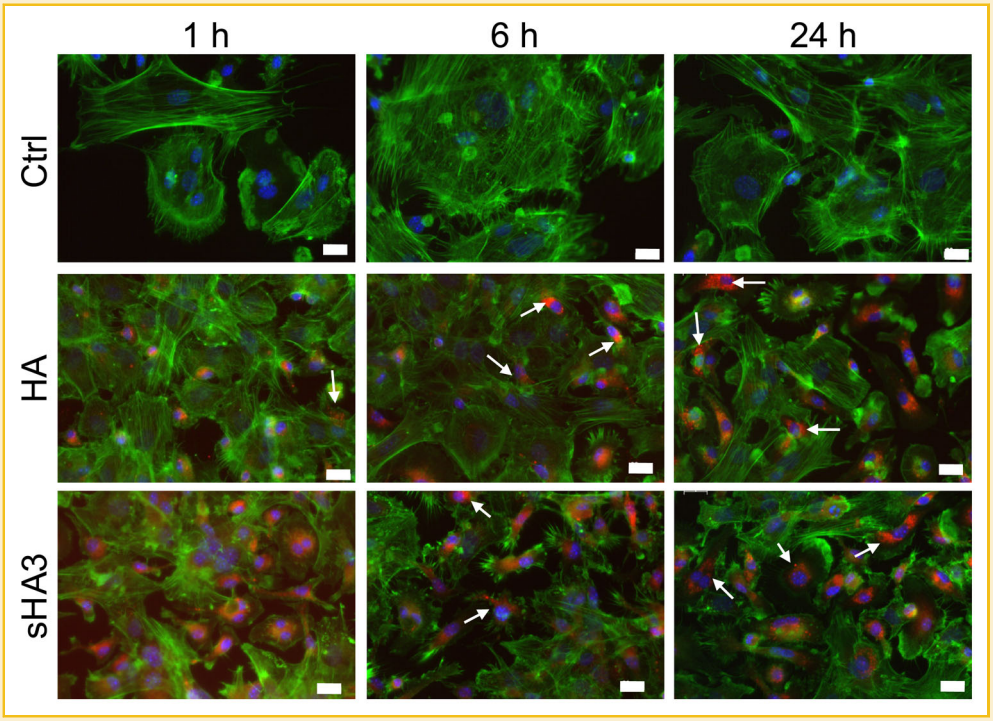

Fig. 2. MSCs are susceptible to fluorescent HAs. Cells seeded on glass slides were exposed to solute red-fluorescent low-molecular HA (HA-ATTO 565) or high-sulfated HA (sHA3-ATTO 565) for 1, 6, or 24 h, respectively. Untreated cells served as controls (Ctrl). Subsequently, slides were stained for F-actin (green) and cell nuclei (blue) and analyzed using digital microscopy. A representative image of three replicates is shown. Magnification: 252×, white bars equate 20 μm, arrows highlight cells with GAG containing vesicles.

and C) compared to GAG-free controls, whereas a slight increase could be observed for apoptosis (Fig. 4D). Sulfate modification led to loss of the proliferative activity of about 40% (Fig. 4B) but at the same time to a nearly complete suppression of necrosis and apoptosis (Fig. 4C and D).

GAG SULFATION INCREASES OSTEOBLASTIC MARKER GENE EXPRESSION

Exposition of differentiating MSCs to GAGs led to changes in the expression of osteoblastic marker genes and corresponding protein levels. Whereas the expression of the OC differentiation factor RANKL was barely detectable on all aECMs, its soluble decoy receptor OPG was profoundly expressed (ELISA, data not shown). Gene expression analysis of cells stimulated with solute GAGs showed a non significant increase in OPG expression in the presence of sulfated, but not native GAGs compared to untreated cells (Fig. 5A). Regulation in response to different GAGs was only observed for ALP (Fig. 5B) and OCN (Fig. 5C), but not Runx2 (data not shown). Both ALP and OCN expression were increased in response to GAG sulfation. However, no differences could be observed between GAGs differing in chain length

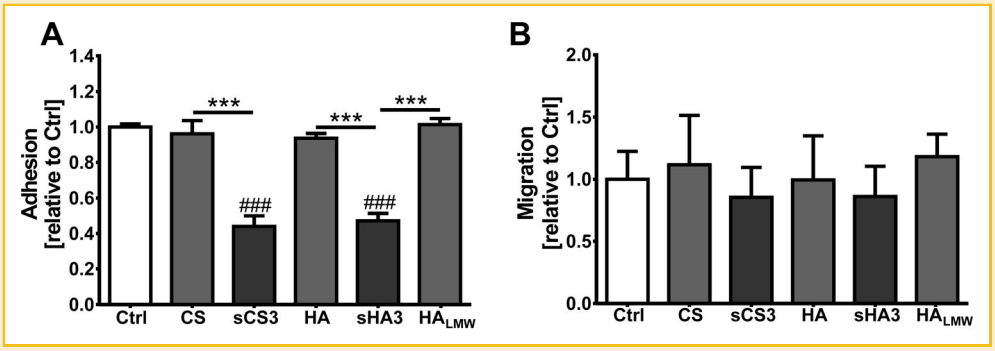

Fig. 3. GAG sulfation inhibits cell adhesion, but not migration of MSCs. (A) Cell adhesion and (B) migration after 72 h of murine MSCs were assessed in response to (A) aECM matrices with GAGs or (B) solute GAGs. All values represent the normalized mean ± SD of n = 3. Abbreviations used: Ctrl, collagen coating/untreated cells; CS native chondroitin sulfate; sCS3, high-sulfated chondroitin sulfate; HA, native hyaluronan; sHA3, high-sulfated hyaluronan; HA_{LMW}, low-molecular weight hyaluronan. $^{###}P < 0.001$ Student's *t*-test versus Ctrl; $^{***}P < 0.001$ Student's *t*-test versus respective treatment.

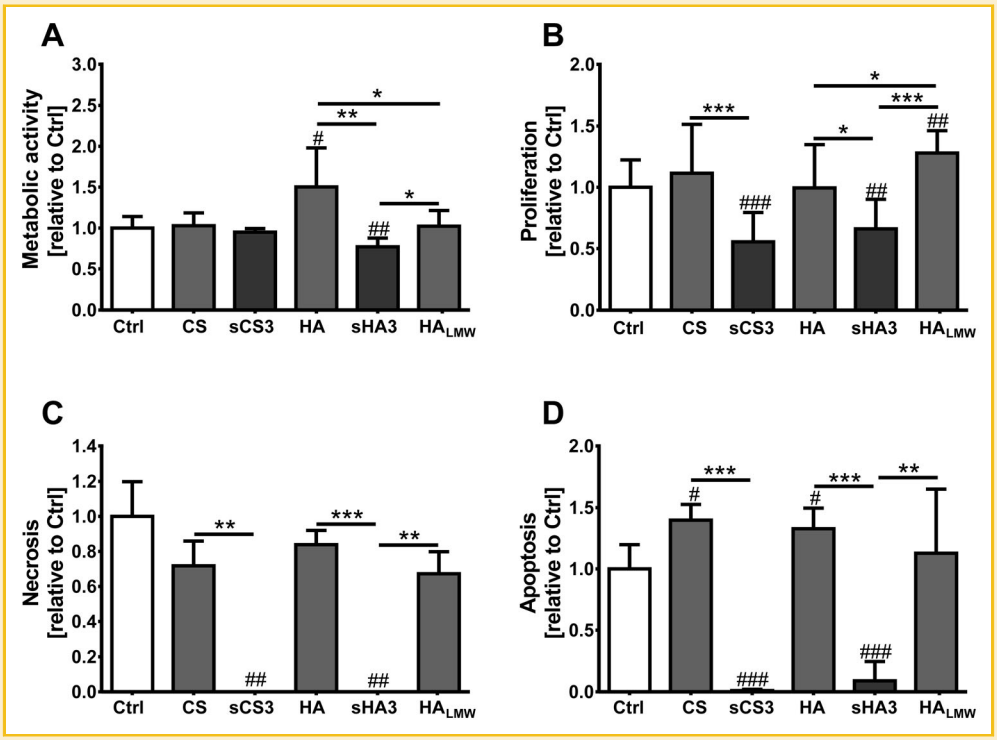

Fig. 4. GAG sulfation modulates MSC viability. (A) Metabolic activity, (B) proliferation, (C) necrosis, and (D) apoptosis of differentiating murine MSCs growing on aECM matrices were assessed at day 5. All values represent the normalized mean ± SD of (A,B) n = 4, (C,D) n = 3–4. Abbreviations used: Ctrl, collagen coating; CS native chondroitin sulfate; sCS3, high-sulfated chondroitin sulfate; HA, native hyaluronan; sHA3 high-sulfated hyaluronan; HA_{LMW}, low-molecular weight hyaluronan. $^{\#}P < 0.05$, $^{\#\#}P < 0.01$, $^{\#\#\#}P < 0.001$ Student's *t*-test versus Ctrl; $^{*}P < 0.05$, $^{**}P < 0.01$, $^{***}P < 0.001$ Student's *t*-test versus respective treatment.

(HA vs. HA_{LMW}) or GAGs of different monosaccharide composition (sHA3 vs. sCS3).

GAG SULFATION RESULTS IN INCREASED MATRIX FORMATION

When differentiating MSCs in osteogenic medium towards OBs, ALP activity and mineralized matrix deposition can be utilized as functional markers to evaluate the progress of maturation. We observed a pronounced increase in ALP activity at day 7 in response to high-sulfated GAGs, but not native GAGs (Fig. 6A). Accordingly, mineralized matrix deposition was not affected in the presence of native GAGs, but nearly abolished in the presence of high-sulfated GAGs (data not shown). However, the culture media utilized for this experiment contained 2 mM Ca^{2+}, which represents the lower range of Ca^{2+} levels in human serum. Since Ca^{2+} concentrations may be higher within local bone microenvironment, especially during bone remodelling, and GAGs are known to chelate cations, we next used higher Ca^{2+} concentrations to better reflect the local situation in bone. We increased the concentration to 10 mM Ca^{2+}, which was

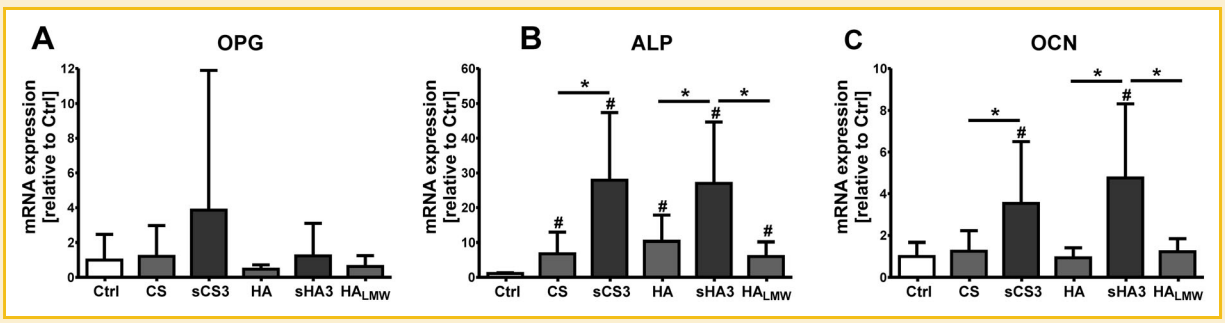

Fig. 5. Sulfation of GAGs increases osteogenic marker gene expression of MSCs. Quantitative real-time PCR analysis of (A) OPG, (B) ALP, and (C) OCN expression levels in differentiating murine MSCs exposed to 200 μg/ml GAGs. All values represent the normalized mean ± SD of (A) n = 4–5, (B) n = 4, (C) n = 3–4. Abbreviations used: Ctrl, untreated cells; CS, native chondroitin sulfate; sCS3, high-sulfated chondroitin sulfate; HA, native hyaluronan; sHA3, high-sulfated hyaluronan; HA_{LMW}, low-molecular weight hyaluronan. $^{\#}P < 0.05$ Student's *t*-test versus Ctrl; $^{*}P < 0.05$, Student's *t*-test versus respective treatment.

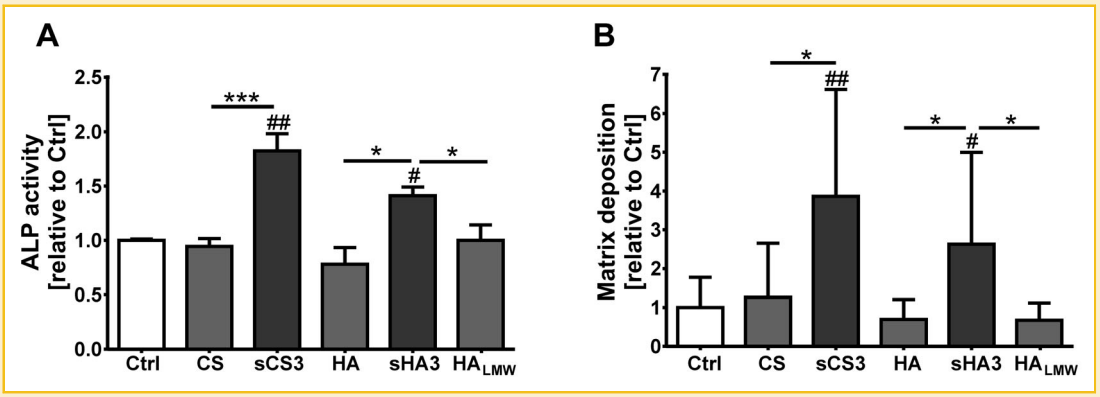

Fig. 6. GAG sulfation promotes OB differentiation and calcium deposition. During osteogenic differentiation of murine MSCs, (A) ALP activity was analyzed after 7 days and (B) calcium deposition was assessed after 21 days. All values represent the normalized mean ± SD of n = 3–4. Abbreviations used: Ctrl, collagen coating; CS, native chondroitin sulfate; sCS3, high-sulfated chondroitin sulfate; HA, native hyaluronan; sHA3, high-sulfated hyaluronan; HA_{LMW}, low-molecular weight hyaluronan. $^{\#}P < 0.05$, $^{\#\#}P < 0.01$, Student's *t*-test versus Ctrl; $^{*}P < 0.05$, $^{***}P < 0.001$ Student's *t*-test versus respective treatment.

previously reported to support matrix deposition without affecting viability [Maeno et al., 2005]. Under these culture conditions, we observed a significant increase in mineral deposition when treated with sulfated GAGs compared to the native GAGs (Fig. 6B) similar to the pro-osteogenic effects observed at mRNA level.

GAG SULFATION IMPAIRS PARACRINE OSTEOBLAST-OSTEOCLAST SIGNALING

Neither OC precursor adhesion (Fig. 7A) nor viability (Fig. 7B), nor motility (Fig. 7C) were affected by supernatants collected from OBs grown on aECMs. In contrast, differentiation was significantly impaired. When treated with the supernatants alone, OC did not form. However, protein analyses of all supernatants via ELISA revealed RANKL concentrations below the detection limit of 16 pg/ml and pronounced OPG release above the ELISA detection limit of 1,200 pg/ml. Hence, when small doses of RANKL (10 ng/ml) were added, differences between the HA derivatives containing aECMs could be revealed (Fig. 7D). OC formation was decreased by supernatants of OB grown on all aECMs investigated, however, the effect was most pronounced on surfaces containing sHA3. The same effect could be observed for OC resorptive activity. OC precursors that were differentiated in the presence of OB supernatants did not resorb SaOS-2-derived matrix. When supplemented with RANKL, all treatment groups showed reduced resorptive activity, which was most pronounced in cells exposed to supernatants derived from wells with matrices containing sHA3. Time dependent differences were apparent only for adhesion and the TRAP staining. Here, progressing differentiation of OBs on aECMs led to a decrease of adhesion of OC precursors that reached significance only at the latest observed differentiation phase (d15-21). The severe inhibition of OC differentiation by sHA3 however gradually diminished over time.

DISCUSSION

Our present study was aimed at characterizing the potential of sulfated GAGs in aECM coatings to improve bone remodeling. Utilizing ECM components to mimic the native microenvironment proved to be a promising approach since aECMs increased the regenerative potential of bone cells by enhancing osteogenesis and concurrently suppressing osteoclastogenesis [Salbach et al., 2012a]. Combinations of Coll and GAGs, two major components of the organic bone ECM, have been investigated for their application for skin, and later also bone regeneration since the 1970s [Spector, 2013] with non conclusive results. Except for HA, the GAGs found in bone can be post-translationally sulfated. Their sulfation patterning is subject to continuous changes during osteogenic differentiation [Haupt et al., 2009; Hoshiba et al., 2009] and development [Mark et al., 1990; Manton et al., 2007] of MSCs suggesting a regulatory role in bone homeostasis. Consistent with this, we could show that differently sulfated HA derivatives interact with mediator proteins relevant to bone healing in a sulfation-dependent manner in previous studies [Hintze et al., 2009, 2012a; Salbach-Hirsch et al., 2013].

Similar to the data found on osteoclasts, existing studies on osteoblast differentiation in response to sulfated GAGs revealed variable effects (reviewed in Salbach et al. [2012b]). This can be attributed partially to the use of non-standardized GAGs. Thus far, GAGs and especially sulfated GAGs are usually obtained from natural sources [Mucci, 2000; Brown and Pummill, 2008]. These GAGs are subject to fluctuations of sulfation degree and pattern due to the variable activities of the different sulfate-introducing sulfotransferases, which limits their clinical translation. To overcome this, we have synthesized GAG derivatives with defined characteristics concerning chain length and degree of sulfation for our aECMs to assess structure-function relationships. In this context, chemical sulfation is attractive, since it follows a controlled mechanism, resulting in sulfated GAGs with defined substitution patterns, whereas the naturally derived high sulfated GAGs show variabilities.

In this study, GAG sulfation resulted in a pro-osteogenic effect similar to studies performed with human cells [Hempel et al., 2012; Hess et al., 2012; Hintze et al., 2012b; Wojak-Cwik et al., 2013] and rat calvarial osteoblasts [Nagahata et al., 2004; Kunze et al., 2010]. This indicates that GAG sulfation affects bone cell differentiation in a controlled species- and model system-independent manner if

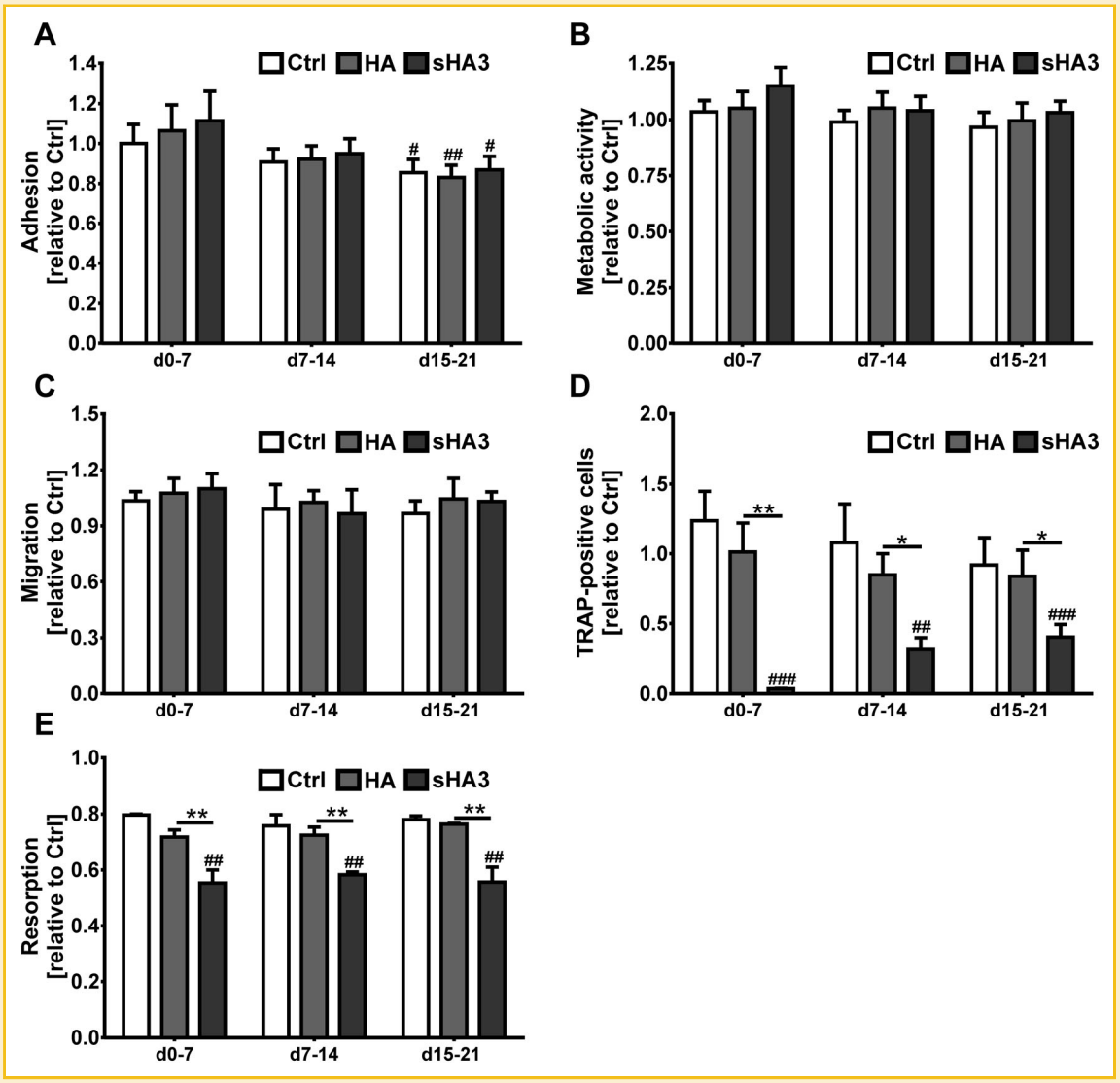

Fig. 7. GAG sulfation impairs the stromal support of osteoclast differentiation. RAW264.7 cells were differentiated with 10 ng/ml RANKL for 3–4 days to generate OC in the presence or absence of OB-derived supernatants. (A) Cell adhesion, (B) metabolic activity, (C) migration, (D) TRAP (TRAP-positive, $\geq$3 nuclei), and (E) resorptive activity on a SaOS-2 cell derived matrix were assessed during differentiation. All values were normalized against cells cultured without supernatants and represent their mean $\pm$ SD of (A, B, D, and E) n = 4, (C) n = 3. Abbreviations used: Ctrl, collagen coating; HA, native hyaluronan; sHA3, high-sulfated hyaluronan. $^{\#}P < 0.05$, $^{\#\#}P < 0.01$, $^{\#\#\#}P < 0.001$ Student's *t*-test versus Ctrl; $^{*}P < 0.05$, $^{**}P < 0.01$, Student's *t*-test versus respective treatment.

comparable polymers are used. To further investigate the underlying mechanisms, we first excluded the probability that GAG sulfation results in impaired uptake that could attribute to all subsequent effects. Therefore, fluorescent derivatives of HA_{LMW} and sHA3 were synthesized. We observed internalized GAGs after 1 h, which, over time, localized to perinuclear vesicles. Of note, this process was faster for the non-sulfated HA. This may indicate a regulated internalization process mediated by the sulfate groups. And indeed, endocytosis regulating proteins were increased in MSCs cultured on sHA3 [Kliemt et al., 2013]. Using unlabeled GAGs, MSC adhesion, but not subsequent migration was affected by the degree of sulfation. This may be due to differences in GAG uptake kinetics, GAG charge, or intracellular processing.

We recognize that this study has potential limitations. The fluorescent GAGs were selected for microscopy primarily for appropriate and stable fluorescence, which did not consider their linking chemistry or molecular weight. Also, different labeling strategies were applied to avoid cross reactions with the previously introduced sulfate groups. Therefore we cannot exclude that the different molecular weights and chemical procedures, side-on vs. end-on functionalization, resulting in a different location of the dye within the GAG and possible changes in GAG characteristics, contribute to the different kinetics. Since the presence of GAGs during the in vitro fibrillogenesis of Coll affects the Coll fibrillar structure [Bierbaum et al., 2012; Hintze et al., 2012b], these changes may also contribute to the outside-in signaling, for example, by modifying the

affinity of Coll to receptors such as integrins. However, morphological changes of the fibrillar structure by variations of the assembly buffer system alone had no effect on cell response [Bierbaum et al., 2012]. Also, studies using Coll type I [Hempel et al., 2012; Büttner et al., 2013], type II [Hintze et al., 2012b], and Coll free systems [Kunze et al., 2010] produced similar results, indicating that GAGs exert their biological effects independently of the presence or the subtype of Coll. Finally, our study was performed in murine cells and clearly will require in vivo validation. However, the evidence of species independent effects of GAG sulfation in OCs [Salbach et al., 2012a] and now OBs strongly suggests a regulatory role in vivo as well.

In osteoclasts GAG sulfation strongly interfered with actin-cytoskeleton reorganization [Salbach et al., 2012a]. Here, MSCs also displayed distinct changes of their actin distribution. While OCs did not form their typical sealing zone actin belt in the periphery, MSCs lacked stress fibers and focal adhesion points. The focal adhesion kinase, and associated GTPase activities regulated in OCs, might be linked to this phenomenon as well [Kliemt et al., 2013].

GAG sulfation resulted in an anti-proliferative effect, which was not associated with increased apoptosis or necrosis. On the contrary, both basal apoptosis and necrosis were very low and nearly non-detectable in response to GAG-sulfation. Also, lower metabolic activity could only partly be attributed to be causative for the decrease in proliferation. Of note, the decreased viability and proliferation did not result in reduced osteogenesis. On the contrary, we found up-regulated osteogenic marker gene expression, ALP activity, and subsequent calcium deposition, indicating a shift from the proliferative stage to a more mature matrix synthesis phenotype.

Here again, variations in Coll fibril morphology may contribute to the observed effects since Coll serves as a template for mineralization. In addition, the process of biomineralization, as described by the polymer-induced liquid-precursor system, entails polypeptides with anionic groups. These anionic polymers sequester calcium ions, which then build up a charge to sequester counter ions [Gower, 2008]. GAGs, and especially sulfated GAGs, exhibit a high number of anionic groups and are known to sequester positively charged ions that may interfere with hydroxyapatite growth [Chen and Boskey, 1985]. By direct interference of high-sulfated GAGs with this process an overall increased mineralization capacity could result in the absence of calcium deposition. This defect in matrix deposition was rescued in the presence of 10 mM calcium, suggesting that calcium concentration may represent a key factor. During MSC differentiation, low calcium concentrations are suitable for proliferation and survival, whereas higher concentrations (6–10 mM) markedly promoted differentiation and mineralization [Maeno et al., 2005]. Also, proteome analysis revealed calcium signaling as one of the highest regulated pathways in response to GAG alterations [Kliemt et al., 2013].

Of note, GAG sulfation interfered with the OB support of osteoclastogenesis. Supernatants derived from OBs on aECM had anti-osteoclastogenic properties, most likely due to the high OPG and low RANKL protein levels. Of note, we observed a gradual increase for TRAP-positive cells when exposed to supernatants of osteoblasts of increasing maturity. However, during MSC differentiation RANKL expression progressively decreased or remained stable whereas OPG expression increased [Hofbauer et al., 1999; Thomas et al., 2001; Atkins et al., 2003]. Since this would translate to an even more pronounced anti-osteoclastogenic effect, the gradually decreasing osteoclastogenesis inhibition may be related to a RANKL/OPG independent mechanism. The aECMs were prepared by in vitro fibrillogenesis without further crosslinking, rendering a gradual release of GAGs and Coll degradation products possible. The GAG release declines over time and may therefore attribute for both the effects on adhesion and the TRAP staining. In our previous study, Coll alone had anti-adhesive potential, whereas sulfated GAGs increased adhesion. Here, a slightly pro-adhesive tendency was observed for the sHA3 supernatant, and an overall decline in adhesion over time that might stem from desorbed GAGs and Coll. Also, a direct stimulation with sulfated GAGs significantly impairs osteoclastogenesis. A decline in desorbing GAG could explain the gradual increase in osteoclast numbers over time. However, previously significant effects were observed only for concentrations above 50 μg/ml, whereas GAG-release by desorption is much smaller.

Additionally, high-sulfated GAGs regulated connexin 43 (Cx43, data not shown), playing a central role in cell-to-cell communication in the skeleton [Plotkin and Bellido, 2013]. This protein is expressed in OBs, osteocytes, and OCs alike and is involved in their inter-cellular coupling. These gap junction proteins allow for exchange of small molecules between bone cells and their extracellular milieu and may be involved in the regulation of the paracrine exchange observed in this study as has been indicated before [Nagahata et al., 2004]. In addition, GAGs show a great variety of interactions with bone-regulating proteins and cytokines such as tumor necrosis factor, TNF-related apoptosis-inducing ligand, bone morphogenetic proteins, OPG, and members of the transforming growth factor-β superfamily. GAGs bound to these proteins can coordinate their activities [Manton et al., 2007; Lamoureux et al., 2009; Salbach-Hirsch et al., 2013] and modulate their bioavailability by sequestration or protection against degradation [Bierbaum et al., 2012].

CONCLUSION

In summary, this study revealed that GAGs are molecules with potent bone-anabolic properties and inhibitory effects on the osteoblast support of osteoclastogenesis, thus displaying a promising potential as a component of diverse bone graft materials. Whether this translates into a favorable profile on bone remodeling at fracture sites requires rigorous in vivo testing.

REFERENCES

Atkins GJ, Kostakis P, Pan B, Farrugia A, Gronthos S, Evdokiou A, Harrison K, Findlay DM, Zannettino ACW. 2003. RANKL expression is related to the differentiation state of human osteoblasts. J Bone Miner Res 18:1088–1098.

Bierbaum S, Douglas T, Hanke T, Scharnweber D, Tippelt S, Monsees TK, Funk RH, Worch H. 2006. Collageneous matrix coatings on titanium implants modified with decorin and chondroitin sulfate: Characterization and influence on osteoblastic cells. J Biomed Mater Res A 77:551–562.

Bierbaum S, Hintze V, Scharnweber D. 2012. Functionalization of biomaterial surfaces using artificial extracellular matrices. Biomatter 2:132–141.

Brown SH, Pummill PE. 2008. Recombinant production of hyaluronic acid. Curr Pharm Biotechnol 9:239–241.

Brydone aS, Meek D, Maclaine S. 2010. Bone grafting, orthopaedic biomaterials, and the clinical need for bone engineering. P I Mech Eng H 224:1329–1343.

Büttner M, Möller S, Keller M, Huster D, Schiller J, Schnabelrauch M, Dieter P, Hempel U. 2013. Over-sulfated chondroitin sulfate derivatives induce osteogenic differentiation of hMSC independent of BMP-2 and TGF-β1 signalling. J Cell Physiol 228:330–340.

Chen CC, Boskey AL. 1985. Mechanisms of proteoglycan inhibition of hydroxyapatite growth. Calcif Tissue Int 37:395–400.

Gower LB. 2008. Biomimetic model systems for investigating the amorphous precursor pathway and its role in biomineralization. Chem Rev 108:4551–4627.

Haupt LM, Murali S, Mun FK, Teplyuk N, Mei LF, Stein GS, van Wijnen AJ, Nurcombe V, Cool SM. 2009. The heparan sulfate proteoglycan (HSPG) glypican-3 mediates commitment of MC3T3-E1 cells toward osteogenesis. J Cell Physiol 220:780–791.

Hempel U, Möller S, Noack C, Hintze V, Scharnweber D, Schnabelrauch M, Dieter P. 2012. Sulfated hyaluronan/collagen I matrices enhance the osteogenic differentiation of human mesenchymal stromal cells in vitro even in the absence of dexamethasone. Acta Biomater Acta Materialia Inc 8:4064–4072.

Hench LL. 1998. Biomaterials: A forecast for the future. Biomaterials 19:1419–1423.

Hess R, Jaeschke A, Neubert H, Hintze V, Moeller S, Schnabelrauch M, Wiesmann H-P, Hart D a, Scharnweber D. 2012. Synergistic effect of defined artificial extracellular matrices and pulsed electric fields on osteogenic differentiation of human MSCs. Biomaterials 33:8975–8985.

Hintze V, Miron A, Moeller S, Schnabelrauch M, Wiesmann H-P, Worch H, Scharnweber D. 2012a. Sulfated hyaluronan and chondroitin sulfate derivatives interact differently with human transforming growth factor-β1 (TGF-β1). Acta Biomater 8:2144–2152.

Hintze V, Miron A, Möller S, Schnabelrauch M, Heinemann S, Worch H, Scharnweber D. 2012b. Artificial extracellular matrices of collagen and sulphated hyaluronan enhance the differentiation of human mesenchymal stem cells in the presence of dexamethasone. J Tissue Eng Regen Med (Epub ahead of print).

Hintze V, Moeller S, Schnabelrauch M, Bierbaum S, Viola M, Worch H, Scharnweber D. 2009. Modifications of hyaluronan influence the interaction with human bone morphogenetic protein-4 (hBMP-4). Biomacromolecules 10:3290–3297.

Hofbauer LC, Gori F, Riggs BL, Lacey DL, Dunstan CR, Spelsberg TC, Khosla S. 1999. Stimulation of osteoprotegerin ligand and inhibition of osteoprotegerin production by glucocorticoids in human osteoblastic lineage cells: Potential paracrine mechanisms of glucocorticoid-induced osteoporosis. Endocrinology 140:4382–4389.

Hoshiba T, Kawazoe N, Tateishi T, Chen G. 2009. Development of stepwise osteogenesis-mimicking matrices for the regulation of mesenchymal stem cell functions. J Biol Chem 284:31164–31173.

Kliemt S, Lange C, Otto W, Hintze V, Möller S, von Bergen M, Hempel U, Kalkhof S. 2013. Sulfated hyaluronan containing collagen matrices enhance cell-matrix-interaction, endocytosis, and osteogenic differentiation of human mesenchymal stromal cells. J Proteome Res 12:378–389.

Kunze R, Rösler M, Möller S, Schnabelrauch M, Riemer T, Hempel U, Dieter P. 2010. Sulfated hyaluronan derivatives reduce the proliferation rate of primary rat calvarial osteoblasts. Glycoconj J 27:151–158.

Lamoureux F, Picarda G, Garrigue-Antar L, Baud′huin M, Trichet V, Vidal A, Miot-Noirault E, Pitard B, Heymann D, Rédini F. 2009. Glycosaminoglycans as potential regulators of osteoprotegerin therapeutic activity in osteosarcoma. Cancer Res 69:526–536.

Livak KJ, Schmittgen TD. 2001. Analysis of relative gene expression data using real-time quantitative PCR and the 2(-Delta Delta C(T)) Method. Methods 25:402–408.

Lutter A-H, Hempel U, Wolf-Brandstetter C, Garbe AI, Goettsch C, Hofbauer LC, Jessberger R, Dieter P. 2010. A novel resorption assay for osteoclast functionality based on an osteoblast-derived native extracellular matrix. J Cell Biochem 109:1025–1032.

Maeno S, Niki Y, Matsumoto H, Morioka H, Yatabe T, Funayama A, Toyama Y, Taguchi T, Tanaka J. 2005. The effect of calcium ion concentration on osteoblast viability, proliferation and differentiation in monolayer and 3D culture. Biomaterials 26:4847–4855.

Manton KJ, Leong DFM, Cool SM, Nurcombe V. 2007. Disruption of heparan and chondroitin sulfate signaling enhances mesenchymal stem cell-derived osteogenic differentiation via bone morphogenetic protein signaling pathways. Stem Cell 25:2845–2854.

Mark MP, Baker JR, Kimata K, Ruch JV. 1990. Regulated changes in chondroitin sulfation during embryogenesis: An immunohistochemical approach. Int J Dev Biol 34:191–204.

Mathieu LM, Mueller TL, Bourban P-EE, Pioletti DP, Muller R, Manson JA, Müller R, Månson J-AE. 2006. Architecture and properties of anisotropic polymer composite scaffolds for bone tissue engineering. Biomaterials 27: 905–916.

Mucci A. 2000. 1H and 13C nuclear magnetic resonance identification and characterization of components of chondroitin sulfates of various origin. Carbohyd Polym 21:37–45.

Nagahata M, Tsuchiya T, Ishiguro T, Matsuda N, Nakatsuchi Y, Teramoto A, Hachimori A, Abe K. 2004. A novel function of N-cadherin and Connexin43: Marked enhancement of alkaline phosphatase activity in rat calvarial osteoblast exposed to sulfated hyaluronan. Biochem Biophys Res Commun 315:603–611.

Pichert A, Samsonov SA, Theisgen S, Thomas L, Baumann L, Schiller J, Beck-Sickinger AG, Huster D, Pisabarro MT. 2012. Characterization of the interaction of interleukin-8 with hyaluronan, chondroitin sulfate, dermatan sulfate and their sulfated derivatives by spectroscopy and molecular modeling. Glycobiology 22:134–145.

Pittenger MF. 2008. Mesenchymal stem cells from adult bone marrow. Methods Mol Biol 449:27–44.

Plotkin LI, Bellido T. 2013. Beyond gap junctions: Connexin43 and bone cell signaling. Bone 52:157–166.

Prince CW, Navia JM. 1983. Glycosaminoglycan alterations in rat bone due to growth and fluorosis. J Nutr 113:1576–1582.

Rauner M, Sipos W, Goettsch C, Wutzl A, Foisner R, Pietschmann P, Hofbauer LC. 2009. Inhibition of lamin A/C attenuates osteoblast differentiation and enhances RANKL-dependent osteoclastogenesis. J Bone Miner Res 24: 78–86.

Robey PG, Boskey AL. 2009. The composition of bone. In: Rosen CJ, editor. Primer on the metabolic bone diseases and disorders of mineral metabolism. Hoboken, NJ, USA: John Wiley & Sons, Inc. pp 32–38.

Salbach J, Kliemt S, Rauner M, Rachner TD, Goettsch C, Kalkhof S, von Bergen M, Möller S, Schnabelrauch M, Hintze V, Scharnweber D, Hofbauer LC. 2012a. The effect of the degree of sulfation of glycosaminoglycans on osteoclast function and signaling pathways. Biomaterials 33:8418–8429.

Salbach J, Rachner TD, Rauner M, Hempel U, Anderegg U, Franz S, Simon J-C, Hofbauer LC. 2012b. Regenerative potential of glycosaminoglycans for skin and bone. J Mol Med 90:625–635.

Salbach-Hirsch J, Kraemer J, Rauner M, Samsonov SA, Pisabarro MT, Moeller S, Schnabelrauch M, Scharnweber D, Hofbauer LC, Hintze V. 2013. The

promotion of osteoclastogenesis by sulfated hyaluronan through interference with osteoprotegerin and receptor activator of NF-κB ligand/osteoprotegerin complex formation. Biomaterials 34:7653–7661.

Schneider CA, Rasband WS, Eliceiri KW. 2012. NIH Image to ImageJ: 25 years of image analysis. Nat Methods 9:671–675.

Spector M. 2013. An interview with I V Yannas. Tracing one of the deepest roots of biomaterials in tissue engineering/regenerative medicine. Biomed Mater 8:040401.

Thomas GP, Baker SU, Eisman JA, Gardiner EM. 2001. Changing RANKL/OPG mRNA expression in differentiating murine primary osteoblasts. J Endocrinol 170:451–460.

Wojak-Cwik IM, Hintze V, Schnabelrauch M, Moeller S, Dobrzynski P, Pamula E, Scharnweber D. 2013. Poly(L-lactide-co-glycolide) scaffolds coated with collagen and glycosaminoglycans: Impact on proliferation and osteogenic differentiation of human mesenchymal stem cells. J Biomed Mater Res A 101:3109–3122.